An Experimental and Computational Study of the Gas-Phase Structures of Five-Carbon Monosaccharides

Leonard P. Guler, Ying-Qing Yu, and Hilkka I. Kenttämaa*

Department of Chemistry, Purdue University, West Lafayette, Indiana 47907-1393

Received: January 30, 2002; In Final Form: May 6, 2002

The gas-phase structures of five five-carbon monosaccharides (D-ribose, D-lyxose, 2-deoxy-D-ribose, D-xylose, and D-arabinose) were studied via ion−molecule reactions with dimethoxyphosphenium ion and 1,3-dioxolane-2-phosphenium ion in a Fourier transform ion cyclotron resonance mass spectrometer. These reagent ions have been earlier demonstrated to be sensitive to the three-dimensional structures of diastereomeric vicinal diols. They were found to display unique reactivity toward each monosaccharide. The results indicate that the gaseous monosaccharides are cyclic molecules. On the basis of a comparison of the reactions of monosaccharides introduced into the gas phase via two different methods, laser-induced acoustic desorption (LIAD) and thermal desorption, the monosaccharides are concluded to maintain their crystalline structure, a pyranose form, throughout the evaporation procedure. For all the monosaccharides in this study except for D-lyxose, the lowest-energy structure found computationally using density functional theory (B3LYP/6-311++G(d,p)) is a pyranose form that lies at least 1.7 kcal/mol lower in energy than the corresponding lowest-energy furanose form. For D-lyxose, however, a furanose form was calculated to be lower in energy than the pyranose form albeit only by 0.1 kcal/mol. These computational results suggest that a pyranose form indeed is likely to be the dominant form of the monosaccharides in the gas phase. Several possible factors controlling the relative stability of each monosaccharide isomer in the gas phase were examined computationally. The order of importance of these factors in determining the relative stabilities was found to be as follows; intramolecular hydrogen bonding interactions ≫ anomeric > steric (axial/equatorial) factors ≫ Δ2 effect.

Introduction

Carbohydrates are the most abundant bioorganic materials on the earth on the basis of mass.[1,2] They play important roles in many biological processes, such as energy storage, neurotransmission, and transfer of genetic information, to name a few.[1,2] Carbohydrate chemistry is of significant interest to the pharmaceutical industry as carbohydrates make up the basis for many drugs and vitamins.[2] Further, many bacterial cell walls are made up from some form of carbohydrates.[2] Monosaccharides are the basic unit of carbohydrates. Yet, several key questions about the structures of monosaccharides remain unanswered. A better understanding of the properties of these building blocks of carbohydrates can drastically improve our understanding of carbohydrate chemistry in general.

NMR studies indicate that in any solution, monosaccharides exist in a complex equilibrium involving a number of isomeric forms.[3] Scheme 1 shows the experimentally determined equilibrium content of the five-carbon monosaccharide D-ribose in aqueous solution.[3] Other NMR studies have shown that the pyranose (six-membered ring) form is the dominant form for most five- and six-carbon monosaccharides.[4−7] These studies have also found a strong dependence of a monosaccharide's structure on the type of solvent.[6,7] For example, in aqueous solution, virtually no molecules with the furanose (five-membered ring) form are detected for D-arabinose, but in dimethyl sulfoxide, as much as 33% of it exists in a furanose form.[6] The current explanation for these compositional differences in the different solvent environments is that water may

SCHEME 1

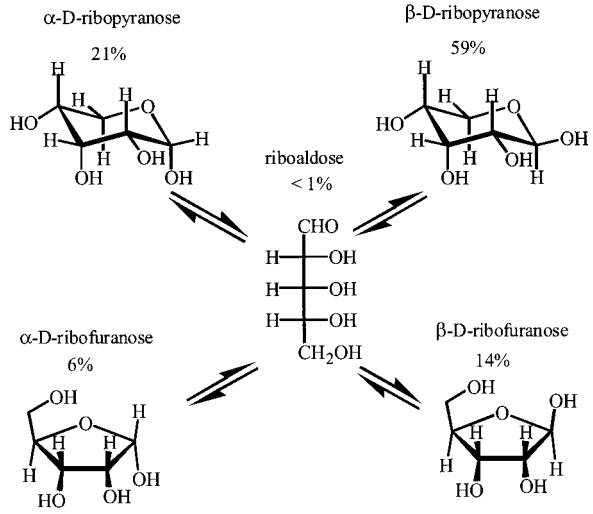

preferentially stabilize the pyranose form through hydrogen bonding, due to its especially good fit into the structure of liquid water.[6,8] Dimethyl sulfoxide, although capable of strong hydrogen bonding in solution, does not preferentially stabilize one sugar form over the other because of the linear arrangement of the solvent molecules.[9] However, the general understanding of the factors that control the equilibrium composition of monosaccharide isomers in solution is limited.[10]

The crystalline structures of most common monosaccharides, including the ones of interest in this study, have been determined via X-ray crystallography and can be obtained from the

* Author to whom correspondence should be addressed. E-mail: hilkka@purdue.edu.

10.1021/jp025577c CCC: $22.00
Published on Web 06/27/2002

Cambridge Crystallographic Files. These data show that all monosaccharides capable of forming a ring are found in the pyranose form.[3]

Structures of the monosaccharides in the gas phase have not yet been examined experimentally. Computational studies[11−28] have generally focused only on the isomers most common in aqueous solution.[10,12−14,17,29] In one of the more complete studies, the energies of many isomers of all six-carbon monosaccharides were examined computationally.[30] In the majority of cases, the energies of the furanose forms were found to be lower than those of the pyranose forms. However, a later study that utilized a larger basis set and correction for the basis set superposition error (BSSE) revealed that the majority of pyranosides have lower energies than the corresponding furanosides.[23]

Only a few computational studies are available on the structures of five-carbon monosaccharides. These studies focused on the furanose forms and their methyl derivatives.[19,22,26−28] No experimental data exist on the gas-phase structures of these monosaccharides. This study focuses on the gas-phase structures of several five-carbon monosaccharides that were studied experimentally using mass spectrometric methods and computationally using the density functional theory.

Experimental Section

The experiments were performed in a Finnigan FTMS 2001 dual-cell Fourier transform ion cyclotron resonance mass spectrometer (FT-ICR) described previously.[31] The instrument consists of a differentially pumped dual-cell reaction chamber aligned collinearly within a magnetic field produced by a superconducting 3.0 T magnet. Both sides of the instrument are equipped with inlets for introduction of liquid samples and with a probe for introduction of solid nonvolatile chemicals. The nominal baseline pressure of each cell is 1×10^{-9} Torr, as measured by an ionization gauge located on each side of the cell. All the monosaccharides were obtained commercially and used as received. The sugar samples were introduced into the instrument via two different methods: thermal desorption and laser-induced acoustic desorption (LIAD). Thermal desorption was achieved by heating the solids probe up to the temperature needed to observe the monosaccharide in the cell, which was typically less than the melting point of the monosaccharide. The nominal pressure in the cell varied for different monosaccharides but typically remained between 2×10^{-8} and 6×10^{-8} Torr.

Details of the LIAD methodology and the LIAD probe used in this study are given elsewhere.[32,33] The samples used in the LIAD experiments were prepared by dissolving about 10 μg of a monosaccharide in 1 mL of methanol, to yield about 10 mM solution of the monosaccharide. Electrospray sample deposition was employed to thinly deposit the samples on the surface of a 10 μm Cu foil.[32] This sample deposition method involves the use of a very high potential difference (6000−10000 V) between the needle of the electrospray and the foil to create a fine mist of charged droplets from the solution containing the sample. On its way to the foil, the solvent is evaporated and the sample thinly covers the foil. This sample deposition technique is fast and can be used to produce very reproducible surface coverages on any conducting surface from solvents that are not highly polar. A monosaccharide sample can be prepared with this technique in less than three minutes.

The reagent ions were produced by electron ionization in one of the cells of the FT-ICR and transferred into the other cell by dropping the potential of the conductance limit (plate separating the cells) to zero volts. Unwanted ions were ejected through the application of a Stored Waveform Inverse Fourier Transform[34] (SWIFT) pulse. The isolated ion of interest was allowed to react for a variable period of time with a desorbed monosaccharide. The total time required to complete the reaction (time at which <10% of reagent ion is left in the cell) was split into eight time intervals and after each, a mass spectrum was measured. At nominal pressures of 2×10^{-8} to 6×10^{-8} Torr, it typically took 10 to 15 s to complete the reaction. Each reaction was repeated several times to ensure that the product branching ratios were reproducible within 10%. A background spectrum was taken for each reaction time by ejecting the reactant ion from the cell and letting the reaction proceed. The background spectrum was then subtracted from the reaction spectrum. The reactions studied follow the expected pseudo-first-order kinetics. This type of data can provide second-order reaction rate constants, which, however, were not of interest in this study.

Computational Methods

All the calculations were performed using the Gaussian 98 software package.[35] Starting structures for higher level calculations where obtained by preoptimization of about two hundred structures by using molecular mechanics (MM2)[36] and semi-empirical methods (AM1).[37] Sixty-eight lowest-energy structures were examined at B3LYP/6-311++G(d,p) level of theory. The final geometries were obtained using density functional theory (DFT) and employing the standard B3LYP functional in conjunction with 6-311++G(d,p) basis set. Several earlier studies have shown that DFT, and especially the B3LYP functional with a moderately high basis set, can very accurately predict the energetic order of monosaccharides.[11,17,30] One study found that adding diffuse functions to the basis set significantly minimizes the basis set superposition error (BSSE).[23] Vibrational frequencies were calculated at the same level to confirm that the calculated structures were true minima, and to obtain zero-point energy (ZPE) corrections. The reported energies do not include a thermal energy correction but include the contribution of ZPE's.

Results and Discussion

Cyclic or Acyclic? Although mostly cyclic in condensed phases and in solution, sugar molecules evaporated into the gas phase may not maintain their cyclic structure throughout the vaporization process. The uncertainty arises from studies that have shown that sugar isomer composition depends strongly on the temperature of the solution.[38] For example, NMR studies on 1-deoxy-D-fructose have shown that 5% of this monosaccharide exists in the acyclic form at room temperature, but 20% at 85 °C.[38] The transformation of one sugar isomer to another is a solvent-mediated process and thus cannot occur once the monosaccharide is in the gas phase.[39] However, it is possible for a cyclic structure to undergo ring opening upon heating during evaporation, especially if the samples are not completely dry.

The issue as to whether monosaccharides are cyclic or acyclic in the gas phase was addressed by examination of the reactivity of the monosaccharides toward two phosphenium ions, the dimethoxyphosphenium cation, and the 1,3-dioxolane-2-phosphenium cation. These particular ions were chosen because of their unique ability to distinguish between cyclic diastereomeric diols, such as *cis*- and *trans*-1,2-cyclopentanediols and *cis*- and *trans*-1,2-cyclohexanediols.[40] The mechanistic details of the reactions of the dimethoxyphosphenium ion are given elsewhere.[40] The proposed mechanisms for the reactions of 1,3-

SCHEME 2

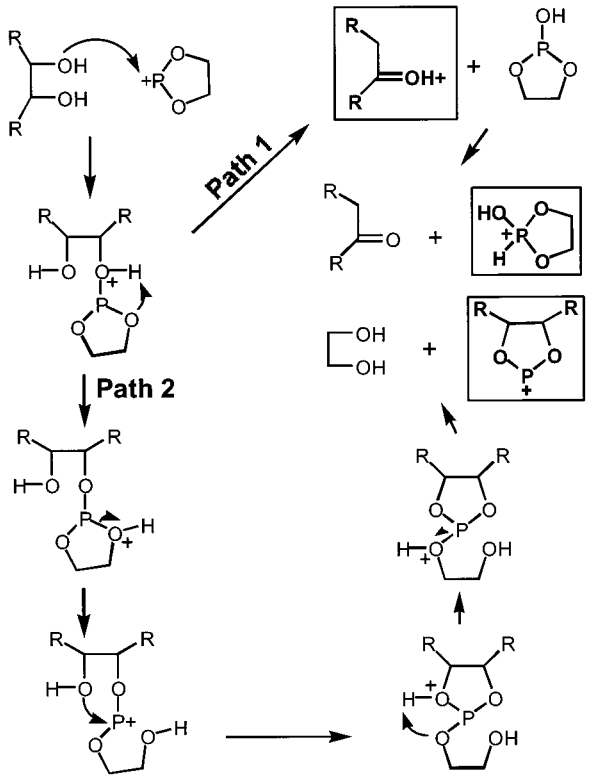

dioxolane-2-phosphenium ion with a diol are shown in Scheme 2. Only two competing pathways were observed for reactions of this ion, i.e., addition followed by the elimination of ethylene glycol, and hydroxide abstraction.

The reactions of the phosphenium ions with alcohols are driven by the exothermicity of the initial addition step that forms the P−O bond. DFT calculations at B3LYP/6-311++G(d,p) level estimate this addition to produce as much as 40 kcal/mol of energy. This energy is available to the gaseous collision complex to overcome reaction barriers leading to the formation of the products. For gas-phase reactions to be observed, their products and the barriers leading to the products must lie lower in energy than the sum of the energies of the separated reactants.

To examine whether the phosphenium ions can be used to differentiate acyclic diastereomers, they were allowed to react with adonitol and L-arabitol (Table 1). These polyfunctional alcohols are acyclic derivatives of monosaccharides. They differ only in the stereochemistry of two chiral carbon atoms. Identical reactivity was observed for each of the ions toward adonitol and L-arabitol (Table 1). This result suggests that diastereomeric acyclic vicinal polyols cannot be differentiated by these phosphenium ions, mainly because of the rotational freedom that the hydroxymethyl groups have in the acyclic polyols. The paths leading to the observed products for 1,3-dioxolane-2-phosphenium ion are analogous to the those shown in Scheme 2. The products formed in the reaction of dimethoxyphosphenium ion with the polyols are analogous to the ones reported earlier for diols[40] and to those shown in Scheme 2.

In the acyclic form, the five-carbon monosaccharides structurally resemble adonitol and L-arabitol in that they both have freely rotating adjacent hydroxymethyl groups. Thus, identical products and product ion abundances are expected for reactions of the phosphenium ions with the acyclic isomeric monosaccharides. However, in their cyclic form, monosaccharides resemble cyclic diols in that each monosaccharide has a distinct number of hydroxyl groups in cis and trans orientations relative to each other, and these orientations are unique for each monosaccharide. Therefore, in cyclic form, monosaccharides may display different reactivity toward the phosphenium ions.

TABLE 1: Reactivity of Two Phosphenium Ions toward Five-Carbon Monosaccharides (structures presented in acyclic form) and Monosaccharide Analogues; Product Ion Masses, Branching Rations, and Identities Are Given

Neutral reagent	H_3CO P+ H_3CO **m/z 93**	O P+ O **m/z 91**
2-deoxy-D-ribose 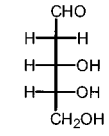	m/z 81 (18%) N[a] - OH, $2H_2O$ m/z 99 (13%) N - OH, H_2O m/z 117 (12%) N - OH m/z 177 (29%) A[b] - H_2O, CH_3OH m/z 195 (7%) A - CH_3OH m/z 227 (21%) A	m/z 81 (14%) N - OH, $2H_2O$ m/z 99 (29%) N - OH, H_2O m/z 109 (5%) H_2O abstraction m/z 117(16%) N - OH m/z 189 (8%) A -$2H_2O$ m/z 207 (13%) A - H_2O m/z 225 (17%) A
D-ribose 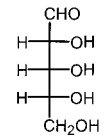	m/z 97 (trace) N - OH, $2H_2O$ m/z 111 (12%) H_2O abstraction m/z 133 (trace) N - OH m/z 179 (15%) A - $2CH_3OH$ m/z 193 (58%) A - H_2O, CH_3OH m/z 207(trace) A -$2H_2O$ m/z 211 (9%) A - CH_3OH m/z 225 (3%) A - H_2O m/z 243 (3%) A	m/z 97 (7%) N - OH, $2H_2O$ m/z 109 (35%) H_2O abstraction m/z 115(22%) N - OH, H_2O m/z 133 (12%) N - OH m/z 179 (10%) A - $(HOCH_2)_2$ m/z 223 (13%) A - H_2O m/z 241(2%) A
D-arabinose 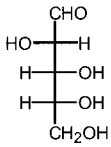	m/z 97 (8%) N - OH, $2H_2O$ m/z 111 (12%) H_2O abstraction m/z 115 (5%) N - OH, H_2O m/z 133 (5%) N - OH m/z 179 (6%) A - $2CH_3OH$ m/z 193 (41%) A - H_2O, CH_3OH m/z 207 (8%) A - $2H_2O$ m/z 211 (7%) A - CH_3OH m/z 225 (6%) A - H_2O m/z 243 (3%) A	m/z 97 (16%) N - OH, $2H_2O$ m/z 109 (32%) H_2O abstraction m/z 115 (25%) N - OH, H_2O m/z 133 (16%) N - OH m/z 223 (8%) A -H_2O m/z 241 (2%) A
D-xylose 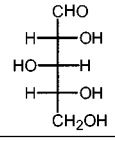	m/z 97 (21%) N - OH, $2H_2O$ m/z 111 (9%) H_2O abstraction m/z 115 (6%) N - OH, H_2O m/z 133 (5%) N - OH m/z 179 (6%) A - $2CH_3OH$ m/z 193 (27%) A - H_2O, CH_3OH m/z 207 (7%) A -$2H_2O$ m/z 225 (13%) A - H_2O m/z 243 (4%) A	m/z 97 (24%) N - OH, $2H_2O$ m/z 109 (24%) H_2O abstraction m/z 115 (31%) N - OH, H_2O m/z 133 (13%) N - OH m/z 223 (6%) A - H_2O m/z 241 (trace) A
D-lyxose 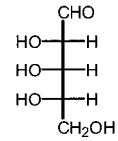	m/z 97 (20%) N - OH, $2H_2O$ m/z 115 (4%) N - OH, H_2O m/z 133 (6%) N - OH m/z 179 (4%) A - $2CH_3OH$ m/z 193 (53%) A - H_2O, CH_3OH m/z 207 (trace) A -$2H_2O$ m/z 211 (6%) A - CH_3OH m/z 225 (3%) A - H_2O m/z 243 (4%) A	m/z 97 (27%) N - OH, $2H_2O$ m/z 115 (24%) N - OH, H_2O m/z 133 (18%) N - OH m/z 179 (11%) A - $(HOCH_2)_2$ m/z 223 (19%) A - H_2O
Adonitol 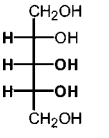	m/z 111 (51%) H_2O abstraction m/z 163 (13%) A - $2CH_3OH$, H_2O m/z 181 (36%) A - $2CH_3OH$	m/z 109 (74%) H_2O abstraction m/z 117 (13%) *N - OH, H_2O m/z 163 (8%) A-$(HOCH_2)_2$, H_2O m/z 181 (5%) A-$(HOCH_2)_2$
L-arabitol 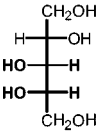	m/z 111 (46%) H_2O abstraction m/z 163 (12%) A - $2CH_3OH$, H_2O m/z 181 (42%) A -$2CH_3OH$	m/z 109 (71%) H_2O abstraction m/z 117 (16%) N - OH, H_2O m/z 163 (9%) A-$(HOCH_2)_2$, H_2O m/z 181 (4%) A-$(HOCH_2)_2$

[a] N = neutral reagent molecule. [b] A = ion complexed with neutral reagent.

The products formed in the reactions of the five-carbon monosaccharides with the two phosphenium ions are shown in Table 1. All the products are analogous to the ones shown in Scheme 2 and described by Thoen and co-workers.[40] Although products of the same *m*/*z* were commonly formed in the course of these reactions, their relative abundances are different for each monosaccharide. The fact that products of same *m*/*z* were formed is not surprising because phosphenium ions react similarly with all alcohols, as was seen in the reactivity of dimethoxyphosphenium ion toward *cis*- and *trans*-1,2-cyclo-

pentanediols and 1,2-cyclohexanediols.[40] The abundances of the products, however, are the real indicators of the structural differences in these molecules. Difference in abundance suggests that barriers leading to the observed products differ for each monosaccharide, which could only be true for molecules that are rigid and have hydroxymethyl groups that cannot freely rotate relative to one another. These criteria could only be satisfied if the monosaccharides have cyclic and hence rigid and distinct structures.

Furanose or Pyranose? As previously mentioned, a pyranose form predominates over the furanose form in a monosaccharide solution for almost all monosaccharides.[4−7] Furthermore, in crystalline form, monosaccharides exist only in pyranose form.[3] However, when monosaccharides are heated to obtain continuous vaporization, their ring structure becomes uncertain. Although monosaccharides cannot undergo transition from a pyranose form to a furanose form in the gas phase because this is a solvent-mediated process, this transition may be possible prior to or during vaporization due to the wetness of the sample.[39]

One of the ways to minimize this process is to use a technique that can desorb neutral molecules very rapidly. One such technique is laser-induced acoustic desorption or LIAD,[33,34] which involves desorbing the sample from a thin metal foil by acoustic waves. A sample for LIAD can be taken from the solid phase into the gas phase in less than 1 ms, which is fast enough to prevent any conformational transitions of monosaccharides prior to desorption. Furthermore, LIAD samples can be prepared very quickly (in less than three minutes), which is necessary to ensure that the monosaccharides maintain their pyranose structures, despite being briefly dissolved in a solvent for electrospray deposition on the metal foil. To better understand the time frame of the isomerization process, let us examine the kinetics of the structural interconversion of monosaccharides.

One can get an estimate of the rate of interconversion between different monosaccharide forms from the phenomenon called mutarotation, a characteristic property of all monosaccharides.[39] Mutarotation is the change in time of the optical rotation that accompanies the interconversion of α- and β- anomers in a solution.[41] Monosaccharides that exist in more than 2% of furanose form at equilibrium (e.g., D-ribose and D-arabinose in water) have complex kinetics associated with their mutarotation and thus belong to the complex mutarotation category.[39] However, mutarotation of monosaccharides that consist of less than 2% of furanose form in solution (e.g., D-glucose, D-lyxose, and D-xylose in water) follows simple first-order kinetics.[39] For sugars that exhibit simple mutarotation, half-lives range from 6.5 min for rhamnose to 48 min for glucose in water at room temperature.[39] The rate of mutarotation can be used as an indicator of how fast one form of a monosaccharide changes into another. There are two types of structural changes that the five-carbon monosaccharides can undergo in solution, transition between the α and the β anomeric forms (Scheme 3), and transition between a furanose and a pyranose form. Both of these transitions require breaking of the carbon−oxygen bond, which is the rate-limiting step. Thus, the simple mutarotation half-lives can be used as a rough indicator of the rate of pyranose-to-furanose transition.

The mutarotation half-lives are strongly dependent on the temperature of the solution as well as the type of solvent used.[39] Solvent acidity also plays an important role on the mutarotation half-life, since protons can catalyze ring opening in monosaccharides and thus speed up mutarotation. Methanol at room temperature was used as the solvent in this study. Since methanol is significantly less acidic than water, the mutarotation half-lives quoted above for water should be longer in the methanol solution. Hence, the short sample preparation times (<3 min) used for LIAD ensured that no significant change in monosaccharide structure took place during the transition from solid to liquid and then back to solid phase.

SCHEME 3

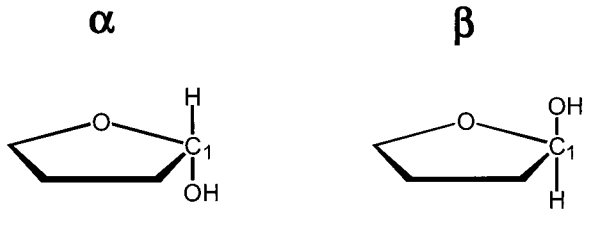

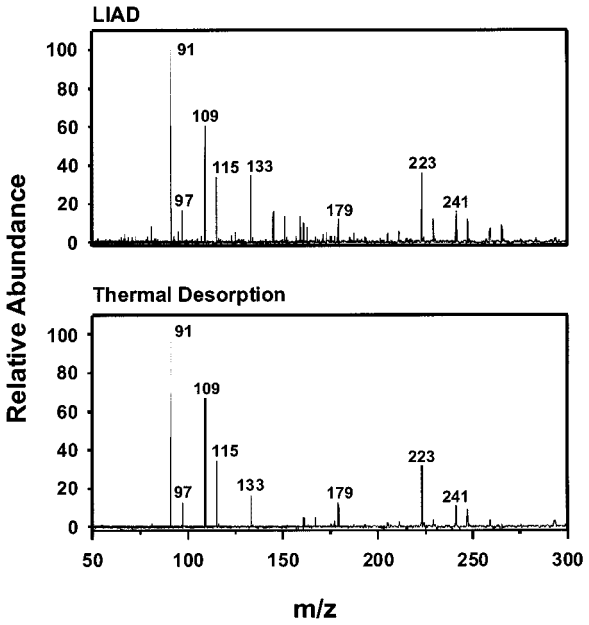

Figure 1. Mass spectra measured to compare the reactions of 1,3-dioxolane-2-phosphenium ion with D-ribose, introduced into the instrument via LIAD (top spectrum), and thermal desorption (bottom spectrum). The small unlabeled peaks are either electrical noise or products formed as a result of secondary reactions.

The monosaccharide samples that were quickly prepared were immediately desorbed into FT-ICR via LIAD, and allowed to react with the 1,3-dioxolane-2-phosphenium ion. On the basis of the preceding discussion, these monosaccharides are expected to have the pyranose structure in the gas phase. Figure 1 shows the comparison of a spectrum measured in one such experiment for D-ribose evaporated by LIAD to that obtained by using thermal desorption. The two spectra are virtually identical. The reactivities of other LIAD desorbed monosaccharides were also identical to those of the thermally desorbed molecules. These results suggest that the monosaccharides introduced via LIAD have the same structure as those introduced thermally, i.e., the pyranose form.

Unfortunately, the mass spectrometric methods used here are not selective enough to further determine the hydroxyl group orientation (α or β) on the anomeric carbon in the monosaccharides. The solid monosaccharide samples contain a mixture of the α- and β-isomers, and the same is probably true for the monosaccharides in the gas phase. However, more sophisticated, spectroscopic methods are required to make a quantitative determination of the α- and β-isomer composition in the gas phase.

Calculations. Computations were employed to examine the relative stabilities of the different structural forms of the five-carbon monosaccharide isomers and the factors that determine their order of stability. Better understanding of these factors will aid in attempts to understand the composition of monosaccharides in the gaseous and condensed phases.

Pyranosides vs Furanosides. Calculations discussed in this paper were performed using density functional theory with the B3LYP hybrid functional and the 6-311++G(d,p) basis set. Table 2[5] summarizes the results of the computational search for the lowest-energy form of each monosaccharide. Sixty-eight monosaccharide structures were examined. Only the lowest-energy structures are shown in Table 2. This table also includes details of hydrogen bonding geometry for each monosaccharide. The results are in good qualitative agreement with the conclusions based on experiments performed in this study, as well as many solution studies.[4−7] For four out of the five monosaccharides examined, a pyranose form was identified as the lowest-energy form, and these differ by at least 1.7 kcal/mol from the lowest-energy furanose form. For the one exception, D-lyxose, the lowest-energy structure was calculated to be furanoside although the energy difference between the lowest-energy furanose and pyranose forms is less than 0.1 kcal/mol. From Table 2 it is also apparent that the number of hydrogen bonding interactions controls the relative stability of the monosaccharide. Without any exceptions, the monosaccharide that has a larger number of hydrogen bonding interactions is lower in energy than the isomer with fewer hydrogen bonding interactions. This result suggests that hydrogen bonding interaction is one of the major factors determining the stability of the monosaccharide isomers in the gas phase. Interestingly, a closer examination of the optimized structures reveals that the majority of the furanosides studied are only capable of having two or fewer intramolecular hydrogen bonding interactions, whereas the majority of pyranosides are capable of having three hydrogen bonds. Adjacent *trans*-hydroxyl groups in furanosides typically do not form a hydrogen bond due to the larger distance separating the OH groups and the high ring strain involved in bringing them closer for interaction. Pyranosides, on the other hand, can form a hydrogen bond between adjacent hydroxyls in both *cis* and *trans* orientation because of the flexibility of the pyranose ring.

Hydrogen Bonding. One of the most important interactions that occur in monosaccharides is intramolecular hydrogen bonding. This interaction is a form of intramolecular solvation, and thus a stabilizing interaction. In monosaccharides, hydrogen bonding refers to an interaction between a hydroxyl hydrogen and an oxygen of another hydroxyl group, typically adjacent to it. To examine the optimal distance of this interaction for unrestricted molecules at the B3LYP/6-311++G(d,p) level of theory, a calculation was performed on two methanol molecules solvated by each other via hydrogen bonding (Scheme 4). Methanol was selected as a simple model of a monosaccharide hydroxymethylene group. The results show that the maximum interaction energy is reached when the hydrogen bond distance (O1H1−O2) is 1.906 Å (Scheme 4). Furthermore, hydrogen bonding is associated with lengthening of the O−H bond in the hydroxyl group whose hydrogen is being shared (Scheme 4). The angle O2H1O1 (175.9°) keeps both oxygen atoms from interacting, thus reducing electron−electron repulsion between them. These are the optimal dimensions for hydrogen bonding of two separate molecules at the B3LYP/6-311++G(d,p) level of theory. The hydrogen bonding distances for monosaccharides (Table 2) are calculated to be typically much longer than 1.906 Å. However, calculations clearly indicate that furanosides have consistently shorter hydrogen bonding distances than pyranosides. The fact that furanosides have hydrogen bonding distances that are more comparable to 1.906 Å suggests that this type of interaction is stronger for furanosides. This finding is not surprising because earlier experimental studies have shown that *cis*-1,2-cyclopentanediol (structurally similar to a furanose form) forms stronger intramolecular hydrogen bonds than *cis*-1,2-cyclohexanediol (structurally similar to a pyranose form). [42]

SCHEME 4

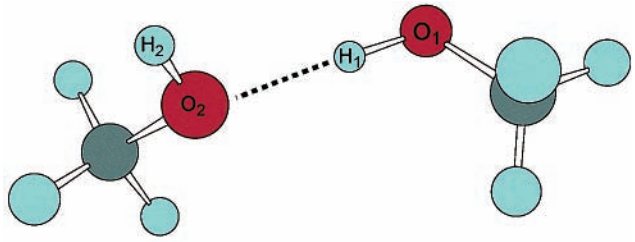

Distance:	O_1—H_1	**is**	**0.970 Å**
Distance:	O_2—H_2	**is**	**0.962 Å**
Distance:	O_1H_1—O_2	**is**	**1.903 Å**
Angle:	$H_2O_2H_1$	**is**	**115.3°**
Angle:	$O_2H_1O_1$	**is**	**175.9°**

SCHEME 5

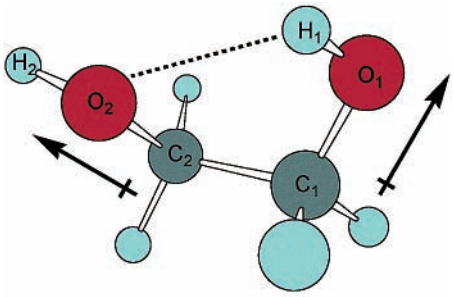

Bond O1H1—O2	**is**	**2.391 Å**
Bond O1—H1	**is**	**0.965 Å**
Bond O2—H2	**is**	**0.961 Å**
Angle O2H1O1	**is**	**106.6 °**
Dihedral O1C1C2O2	**is**	**61.8 °**

The much longer hydrogen bond lengths in monosaccharides than between two methanol molecules can be rationalized by steric restrictions. To better understand these steric interactions, let us examine the calculated geometry of another model, ethylene glycol. Ethylene glycol was chosen because its two hydroxyl groups on two adjacent carbons can interact similarly as the hydroxyl groups of furanosides and pyranosides (Scheme 5). The optimized structure in Scheme 5 reveals a hydrogen bonding interaction similar to the interactions present in monosaccharides. The distance of the hydrogen bond (O1H1−O2) was calculated to be 2.391 Å. This distance is much longer than that obtained for hydrogen bonding interaction of two methanol molecules (1.906 Å). The distance of 1.906 Å could be obtained for ethylene glycol by decreasing the dihedral angle between the two hydroxyl groups but it is prevented by increasing steric repulsions between the eclipsing OH groups and hydrogens. Furthermore, an unfavorable local dipole interaction (Scheme 5) grows stronger as the dihedral angle between the OH groups becomes smaller. Thus, the optimized structure of ethylene glycol is a compromise between having a

TABLE 2: Shown for Each Isomer Are the Energies Relative to the Energy of the Lowest-Energy Isomer (in kcal/mol) at 0 K, Absolute Energies in Hartrees, and Zero-Point Energies (ZPE) in Hartrees (all at B3LYP/6-311++G(d,p)); Also Shown Are the Lengths of the Hydrogen Bonds, and of the O−H Bonds as well as the Dihedral Angles between the Hydroxyl Groups Involved in Hydrogen Bonding

	Relative E Calculated E ZPE	H-bond OxHx—Oy	Ox—Hx[a] distance Å	Hx—Oy[a] distance Å	OxCxCyOy[a] dihedral
 D-β-arabinopyranose	***0*** -572.8364006 0.164735	O2H2—O1 O3H3—O2 O4H4—O3	2.268 2.430 2.256	0.967 0.965 0.966	54.5 61.9 53.0
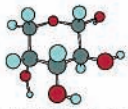 D-α-arabinopyranose	***1.1*** -572.8337555 0.163907	O2H2—O1 O3H3—O2 O4H4—O3	2.537 2.409 2.246	0.964 0.965 0.966	62.7 63.6 52.1
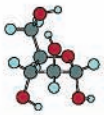 D-α-arabinofuranose	***2.2*** -572.8326379 0.164474	O2H2—O5 O3H3—O1	1.943 2.173	0.972 0.967	10.2[b] 2.5[b]
 D-β-arabinofuranose	***2.8*** -572.830983 0.163778	O2H2—O1 O1H1—O5	2.186 1.964	0.969 0.974	38.9 8.3[b]
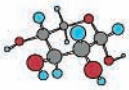 D-α-xylopyranose	***0*** -572.8363285 0.164476	O2H2—O1 O3H3—O2 O4H4—O3	2.232 2.507 2.444	0.967 0.965 0.964	52.4 63.0 64.0
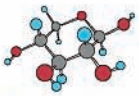 D-β-xylopyranose	***0.5*** -572.8348085 0.163769	O2H2—O1 O3H3—O2 O4H4—O3	2.542 2.481 2.456	0.964 0.964 0.965	65.8 64.9 65.3
 D-β-xylofuranose	***3.6*** -572.8302674 0.164272	O1H1—O3 O3H3—O5	2.202 1.920	0.969 0.972	4.9[b] 12.3[b]
 D-α-xylofuranose	***3.7*** -572.8299573 0.163767	O1H1—O2 O3H3—O5	2.055 1.916	0.969 0.971	30.3 17.5[b]
 D-β-ribopyranose	***0*** -572.8360308 0.165051	O2H2—O4 O3H3—O2 O4H4—O3	2.173 2.205 2.423	0.970 0.967 0.965	2.5[b] 49.0 52.5
 D-α-ribopyranose	***0.3*** -572.8348687 0.164399	O2H2—O1 O3H3—O4 O4H4—O2	2.255 2.399 2.043	0.966 0.966 0.969	55.0 53.3 3.0[b]

TABLE 2 (Continued)

 D-α-ribofuranose	***2.0*** -572.8320657 0.164293	O2H2—O1 O3H3—O2 O1H1—O3	2.174 2.322 2.301	0.968 0.967 0.970	35.9 39.3 1.2[b]
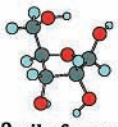 D-β-ribofuranose	***4.3*** -572.8285309 0.164374	O2H2—O3 O5H5—O1	2.023 1.970	0.969 0.970	23.0 38.6[b]
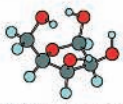 D-β-lyxofuranose	***0*** -572.8361472 0.165789	O1H1—O5 O2H2—O1 O3H3—O2 O5H5—O3	1.878 2.031 2.032 2.005	0.98 0.973 0.972 0.969	13.1[b] 27.4 16.2 50.2[b]
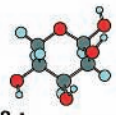 D-β-lyxopyranose	***0.1*** -572.8341998 0.163988	O2H2—O1 O3H3—O2 O4H4—O3	2.241 2.228 2.476	0.965 0.967 0.965	51.6 52.0 63.6
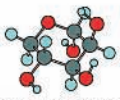 D-α-lyxopyranose	***0.7*** -572.8338843 0.164665	O3H3—O2 O4H4—O3	2.304 2.470	0.967 0.965	52.9 63.8
 D-α-lyxofuranose	***1.4*** -572.8327885 0.164646	O2H2—O3 O3H3—O5	2.187 1.911	0.967 0.973	26.2 49.5[b]
 2-deoxy-D-α-ribopyranose	***0*** -497.5942394 0.160599	O3H3—O1 O4H4—O3	2.033 2.210	0.968 0.968	1.7[b] 49.3
 2-deoxy-D-β-ribopyranose	***1.2*** -497.5917555 0.16006	O3H3—O4	2.283	0.967	52.8
 2-deoxy-D-α-ribofuranose	***1.7*** -497.5903842 0.159414	O3H3—O1	2.263	0.967	4.7[b]
 2-deoxy-D–β–ribofuranose	***3.3*** -497.5866829 0.158228	O5H5—O1	2.541	0.966	7.2

[a] Numbering scheme used for bond lengths and dihedral angles.

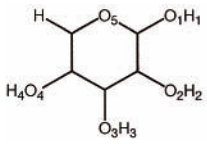

[b] Hydroxyl groups not bonded to the adjacent carbons.

SCHEME 6

maximum effect from the stabilizing hydrogen bonding interactions and a minimum effect from destabilizing steric and dipole interactions.

Both the eclipsing steric repulsion between hydroxyl groups and the unfavorable local dipole interaction (Scheme 5) counteract the stabilizing hydrogen bonding interaction in pyranosides and furanosides. In fact, the cyclic structure of these molecules sterically limits the degree of rotation between two adjacently bound hydroxyl groups, thus causing a decrease in dihedral angle between these groups. This decrease in the dihedral angle between two hydroxyl groups can be seen in Table 2. The results in Table 2 also show that for all pyranose rings, the dihedral angles between the adjacent hydroxyl groups involved in hydrogen bonding are much greater than those in furanose rings. In fact, the pyranosides' dihedral angles as well as hydrogen bonding distances are much more comparable to the dihedral angles and distances calculated for ethylene glycol, than those of furanosides. This observation suggests that for pyranosides, the unfavorable steric interactions will have a lesser effect on the overall stability than in furanosides. Some specific examples in Table 2 also support this point. For example, D-β-lyxofuranose has four seemingly very strong (short) hydrogen bonding interactions. However, the dihedral angles between the adjacent hydrogen bonding hydroxyl groups are very small. The nearly eclipsing geometry of these hydroxyl groups causes a significant steric repulsion between these groups as well as other groups in this molecule. This is the reason this molecule is only slightly lower in energy than the pyranoside isomers of D-ribose, despite the stronger (shorter) hydrogen bonds. Another example of greater steric interactions in furanosides can be seen in two isomers of D-ribose. D-β-Ribopyranose was calculated to be the lowest-energy isomer of D-ribose. However, D-α-ribofuranose, although it has the same number of hydrogen bonding interactions as D-β-ribopyranose, was calculated to lie about 2 kcal/mol higher in energy. This energy difference is likely to be caused by the greater steric interactions in D-α-ribofuranose, arising from the unfavorable dihedral angles between the adjacent hydroxyl groups that are much smaller than those of D-β-ribopyranose.

Pyranoside Stability. Let us now examine the factors that control the relative stabilities of pyranosides since they appear to be the dominant form of monosaccharides in the gas phase. The pyranose form of a sugar can have two distinct chair forms, $^1C_4$ and $^4C_1$ (Scheme 6), in addition to many other higher-energy conformers. Table 3 shows energy comparison between the two lowest-energy pyranoside chair forms for each of the monosaccharide conformers. Out of the five α-monosaccharides studied, three prefer a $^4C_1$ chair and two prefer a $^1C_4$ chair form. On the other hand, three of the β-monosaccharides have a $^1C_4$ chair as their lowest-energy conformer. This slight preference of β-monosaccharides for $^1C_4$ chairs and of α-monosaccharides for $^4C_1$ chairs may be due to the anomeric effect, or the preference for the axial orientation of electronegative substituents at C1 in heterocycles (Scheme 7).[43]

SCHEME 7

0 1 kcal/mol

SCHEME 8

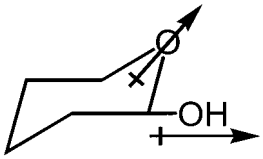

SCHEME 9

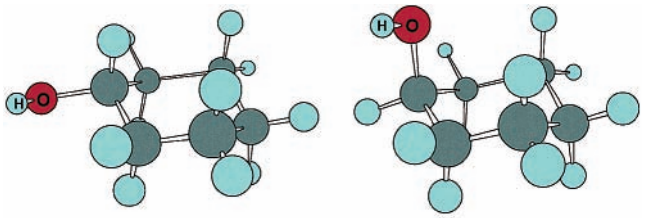

0 **0.9 kcal/mol**

Currently two widely accepted models exist for the anomeric effect. According to the electrostatic model, there is an unfavorable dipole interaction when the hydroxyl group is in the equatorial orientation (Scheme 8). According to the double-bond/no-bond model, there is an energetically favorable stabilization attributed to delocalization of the antiperiplanar lone-pair orbital on oxygen to the antibonding orbital of the carbon−oxygen bond.[43] An energy comparison of the molecules depicted in Scheme 7 revealed that the anomeric effect contributes about 1 kcal/mol to the stability of that molecule. All the α-monosaccharides that exist in the $^4C_1$ chair form and all the β-monosaccharides that exist in the $^1C_4$ chair form have the hydroxyl group on carbon 1 in the axial orientation and thus enjoy special stabilization according to the anomeric effect theory. However, not all the monosaccharides where this stabilizing effect occurs are of lower energy. For four out of 10 pyranosides (includes α and β), the anomeric effect is not strong enough to overcome other known factors that determine the relative stability of monosaccharides, such as intramolecular hydrogen bonding, steric factors and $\Delta 2$ effect. The discussion below will examine some of these factors.

Effect of Steric Factors on Pyranoside Stability. The steric factors mentioned above are different from the ones discussed in relation to pyranose vs furanose rings. These latter steric factors are associated with axial and equatorial orientation of the side groups on the pyranose ring. To approximate the energy difference between an axially oriented hydroxyl group and equatorially oriented hydroxyl group at B3LYP/6-311++G(d,p) level of theory, a calculation was performed on two cyclohexanol molecules. A cyclohexanol with an axial hydroxyl group is calculated to lie about 0.9 kcal/mol higher in energy than one with an equatorial hydroxyl group (Scheme 9). Table 3 summarizes the ratios of the number of equatorial to axial hydroxyl groups for each chair form of each monosaccharide (excluding the hydroxyl group on the anomeric carbon). With the exception of D-α-ribopyranose and D-β-ribopyranose, all the lowest-energy chair forms have a greater or equal number of

TABLE 3: Comparison of the Relative Energies and the Energy-Controlling Factors for the Two Lowest-Energy Pyranoside Conformers

	ring type[a]	relative energy[b]	no. of H-bonds[c]	anomeric effect[d]	equatorial/ axial[e]	Δ2 effect[f]
D-β-lyxopyranose	$^4C_1$	0	3	−	2/1	+
D-β-lyxopyranose	$^1C_4$	2.1	2	+	1/2	−
D-α-lyxopyranose	$^4C_1$	0	2	+	2/1	NA
D-α-lyxopyranose	$^1C_4$	1.0	2	−	1/2	NA
D-β-xylopyranose	$^4C_1$	0	3	−	3/0	NA
D-β-xylopyranose	$^1C_4$	3.7	2	+	0/3	NA
D-α-xylopyranose	$^4C_1$	0	3	+	3/0	−
D-α-lyxopyranose	$^1C_4$	4.9	2	−	0/3	+
D-β-arabinopyranose	$^4C_1$	2.9	2	−	1/2	+
D-β-arabinopyranose	$^1C_4$	0	3	+	2/1	−
D-α-arabinopyranose	$^4C_1$	1.3	2	+	1/2	NA
D-α-arabinopyranose	$^1C_4$	0	3	−	2/1	NA
2-deoxy-D-β-ribopyranose	$^4C_1$	1.3	1	−	1/1	NA
2-deoxy-D-β-ribopyranose	$^1C_4$	0	1	+	1/1	NA
2-deoxy-D-α-ribopyranose	$^4C_1$	0	2	+	1/1	NA
2-deoxy-D-α-ribopyranose	$^1C_4$	4.6	1	−	1/1	NA
D-β-ribopyranose	$^4C_1$	6.5	2	−	2/1	NA
D-β-ribopyranose	$^1C_4$	0	3	+	1/2	NA
D-α-ribopyranose	$^4C_1$	0.1	3	+	2/1	−
D-α-ribopyranose	$^1C_4$	0	3	−	1/2	+

[a] See Figure 5. [b] Energy relative to the lowest-energy isomer. [c] The number of intramolecular hydrogen bonding interactions. [d] "+" means that the hydroxyl group on the anomeric carbon is axial, "−" means that it is equatorial (see Figure 6). [e] no. of hydroxyl groups in equatorial position/ no. in axial position. [f] "+" means that the D2 effect applies, "−" means that it is possible but does not apply to the structure, NA means that it cannot occur (see Figure 9).

SCHEME 10

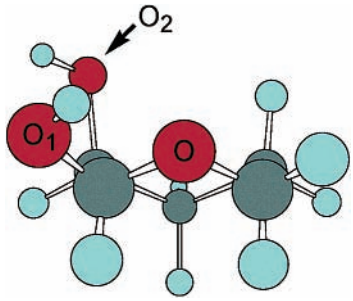

equatorial groups than axial groups. These results suggest that steric effect seems to play a significant role in pyranose ring stability.

Δ2 Effect on Pyranoside Stability. The Δ2 effect is another factor that is thought to control the relative stability of monosaccharide conformers.[30] The Δ2 effect is a form of a steric effect where an element of instability is caused by hydroxyl oxygen (O2) bisecting the angle formed by the ring oxygen atom and an oxygen atom (O1) on an adjacent carbon (Scheme 10).[44] This effect, however, applies only to certain monosaccharides because only specific forms of a monosaccharide can encounter this orientation of atoms. Table 3 shows that this effect can occur for four out of 10 pyranosides studied here. In half of the cases, this destabilizing effect occurs in the more stable isomers, which suggests that the Δ2 effect plays a minor role in determining the relative stability of monosaccharides.

As mentioned above, intramolecular solvation, i.e., intramolecular hydrogen bonding, is another stabilizing factor in the gas phase. For pyranosides, the chair that has the largest number of hydrogen bonding interactions is without an exception lower in energy than a chair that has less of these interactions (Table 3). Although the hydrogen bonding interaction seems to be the dominant factor in determining pyranose stability, a better method of comparison can help to get a semiquantitative understanding of its dominance. The discussion below outlines the quantitative comparisons of each of these factors.

SCHEME 11

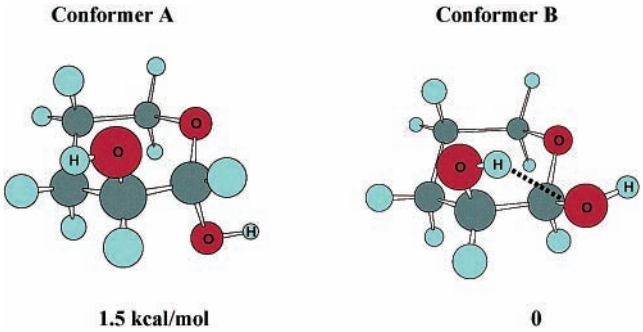

Hydrogen Bonding or Anomeric Effect and Δ2 Effect? Two model compounds, the *cis*- and *trans*-2,3-tetrahydropyrandiols, were examined computationally to get a semiquantitative estimate for the relative importance of the anomeric effect, the Δ2 effect, and hydrogen bonding interaction in determining the stabilities of the molecules. Both of the molecules (Scheme 11) were optimized at the B3LYP/6-311++G(d,p) level. Conformer A (*trans*-2,3-tetrahydropyrandiol) in Scheme 11 has a hydroxyl group on carbon 1 oriented axially, which is favored according to the anomeric effect. However, it has no hydrogen bonding interactions. The conformer B (*cis*-2,3-tetrahydropyrandiol) in Scheme 11 has the hydroxyl group on carbon 1 in the equatorial position which is unfavored according to the anomeric effect. This conformer is also destabilized by the Δ2 effect. However, it has a hydrogen bonding interaction between the two hydroxyl groups. According to calculations, conformer B is 1.5 kcal/mol lower in energy than conformer A. This result suggests that the hydrogen bonding interaction is significantly more important than the anomeric effect and the Δ2 effect combined.

Hydrogen Bonding or Steric Interactions? To determine which has a greater effect on the overall stability of pyranosides, steric (axial/equatorial) factors or intramolecular hydrogen bonding, two conformers of the *cis*-1,3-cyclohexanediol (shown in Scheme 12) were computationally examined. One of the conformers has both hydroxyl groups oriented equatorially

SCHEME 12

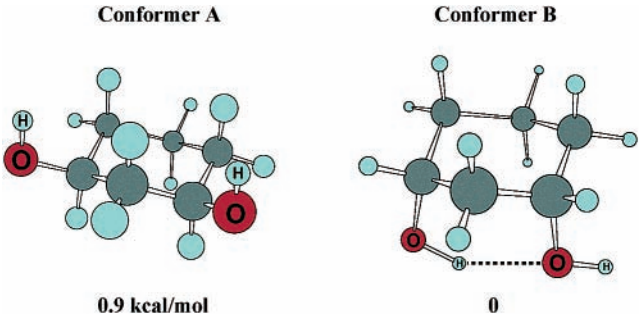

SCHEME 13

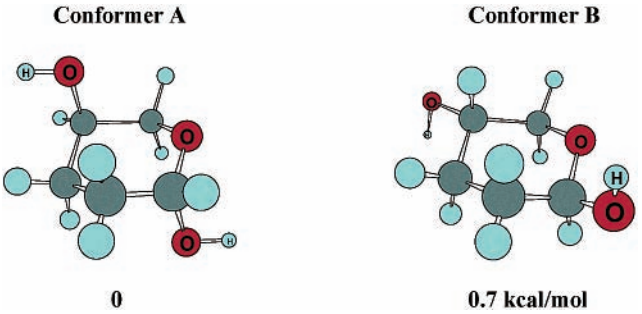

(sterically more preferred). In this conformer, however, two hydroxyl groups are sterically prevented from interacting via hydrogen bonding. The other conformer has two axially oriented hydroxyl groups (sterically less preferred). The orientation of the hydroxyl groups in this conformer allows hydrogen bonding interaction. Once again, the conformer that has a hydrogen bonding interaction was found to be slightly lower in energy (0.7 kcal/mol) than the conformer that has all-equatorial hydroxyl group orientation. This finding suggests a greater contribution to the relative stability of a conformer from the intramolecular hydrogen bonding than from the steric (axial/equatorial) factors.

Steric Interactions or Anomeric Effect? To determine whether the anomeric effect or the steric (axial/equatorial) factors is a greater contributor to the relative stability of pyranosides, the two conformers of *trans*-2,5-tetrahydropyrandiol shown in Scheme 13 were computationally examined. Conformer A in Scheme 13 has the hydroxyl group on carbon 1 oriented axially (preferable for the anomeric effect) and the hydroxyl group on carbon 4 oriented axially (sterically less preferred). On the other hand, conformer B has a hydroxyl group on carbon 1 in an equatorial orientation (not preferable by anomeric effect) and a hydroxyl group on carbon 4 also in equatorial orientation (sterically more preferred). According to the calculations, the conformer that is stabilized by anomeric effect (conformer A) is about 0.7 kcal/mol lower in energy than the conformer B that has an equatorial hydroxyl group orientation (sterically more preferred). This result suggests that the anomeric effect is the second-most important factor in determining the pyranoside stability, whereas steric (axial/equatorial) effect is third and intramolecular hydrogen bonding is most important. Although suitable models to determine quantitatively the contribution of $\Delta 2$ effect could not be found, the results of calculations in this study suggest that $\Delta 2$ effect contributes very little, if anything, to the overall stability of monosaccharides.

Conclusions

Examination of ion−molecule reactions of stereoselective phosphenium ions with five-carbon monosaccharides indicates that the thermally vaporized monosaccharides have the pyranosyl form in the gas phase. The pyranose form is also the dominant form of these sugars in the condensed phases.[4−8] The computational analysis performed using B3LYP/6-311++G(d,p) level of theory for each gaseous monosaccharide isomer is in qualitative agreement with the experimental findings. With one exception (D-lyxose), all of the monosaccharides studied computationally appear to prefer the pyranose form in the gas phase by at least 1.7 kcal/mol. For D-lyxose, the furanose and the pyranose forms are essentially isoenergetic. Further analysis of the computational results revealed that the hydrogen bonding interaction has the dominant control over the relative stabilities of the different forms of the monosaccharides in the gas phase. Furthermore, for pyranosides, the hydrogen bonding interaction has a much greater contribution to the overall energy of the monosaccharide than the anomeric effect, steric (equatorial/axial) factors, or $\Delta 2$ effect. The relative importance of each of these factors was found to be as follows: hydrogen bonding $\gg$ anomeric effect $>$ steric effect $\gg \Delta 2$ effect. Calculations also suggest that although furanosides are capable of stronger (shorter) intramolecular hydrogen bonding, the smaller dihedral angle between adjacent hydroxyl groups cancels some of that stabilizing interaction with increased steric interactions. Due to steric limitations of the furanose ring, the majority of the five-carbon furanosides are capable only of forming two intramolecular hydrogen bonds, whereas the majority of the pyranosides can form three such bonds.

The above results suggest that pyranosides are thermodynamically more stable than furanosides. This in itself, rather than solvation effects,[6,8] could be the reason for monosaccharides preferring pyranoside structures in solution.

Acknowledgment. We thank Chris J. Petzold for help with the LIAD experiments and Melissa F. Mrozek for characterization of the elctrosprayed samples. We also gratefully acknowledge NIH for financial support of this work.

References and Notes

(1) Moran, L. A.; Scrimgeour, K. G.; Horton, H. R.; Ochs, R. S.; Rawn, J. D. *Biochemistry*, 2nd ed.; Neil Patterson Publishers/Prentice-Hall, Inc.: Englewood Cliffs, NJ, 1994.
(2) Pigman, W.; Horton, D. *The Carbohydrates: Chemistry and Biochemistry*; Academic Press: New York, 1972.
(3) Harmon, R. E. *Asymmetry in Carbohydrates*; New York, 1979.
(4) Perlin, A. S. *Can. J. Chem.* **1966**, *44*, 539.
(5) Dias, P.; Perlin, A. S. *Carbohydr. Res.* **1987**, *169*, 159.
(6) Mackie, W.; Perlin, A. S. *Can. J. Chem.* **1966**, *44*, 2039.
(7) Angyal, S. J. *Carbohydr. Res.* **1994**, *263*, 1.
(8) Kabayama, M. A.; Peterson, D. *Can. J. Chem.* **1958**, *36*, 563.
(9) Schlafer, H. L.; Schanffernicht, W. *Angew. Chem.* **1958**, *36*, 563.
(10) Barrows, S. E.; Dulles, F. J.; Cramer, C. J.; French, A. D.; Truhlar, D. G. *Carbohydr. Res.* **1995**, *276*, 219.
(11) Chung-Phillips, A.; Chen, Y. Y. *J. Phys. Chem. A* **1999**, *103*, 953.
(12) Brown, J. W.; Wladkowski, B. D. *J. Am. Chem. Soc.* **1996**, *118*, 1190.
(13) Jebber, K. A.; Zhang, K.; Cassydy, C. J.; Chang-Phyllips, A. *J. Am. Chem. Soc.* **1996**, *118*, 10515.
(14) Eijck, P. B. v.; Hooft, R. W. W.; Kroon, J. *J. Phys. Chem.* **1993**, *97*, 12093.
(15) Glennon, T. M.; Zheng, Y.-J.; Le Grand, S. M.; Shutzberg, B. A.; Merz, K. M. *J. Comput. Chem.* **1994**, *15*, 1019.
(16) Serianni, A. S.; Wu, J.; Carmichael, I. *J. Am. Chem. Soc.* **1995**, *117*, 8645.
(17) Csonka, G. I.; Elias, K.; Csizmadia, I. G. *Chem. Phys. Lett.* **1996**, *257*, 49.
(18) Polavarapu, P. L.; Ewig, C. S. *J. Comput. Chem.* **1992**, *13*, 1255.
(19) Evdokimov, A. G.; Kalb, J.; Koetzle, T. F.; Klooster, W. T.; Martin, J. L. *J. Phys. Chem. A* **1999**, *103*, 744.
(20) Cloran, F.; Carmichael, I.; Serianni, A. S. *J. Phys. Chem. A* **1999**, *103*, 3783.
(21) French, A. D.; Dowd, M. K.; Reilly, P. J. *J. Mol. Struct. (THEOCHEM)* **1997**, *395*−*396*, 271.

(22) Gordon, M. T.; Lowary, T. L.; Hadad, C. M. *J. Am. Chem. Soc.* **1999**, *121*, 9682.
(23) Lii, J.-H.; Ma, B.; Allinger, N. L. *J. Comput. Chem.* **1999**, *20*, 1593.
(24) Dowd, M. K.; French, A. D.; Reilly, P. J. *Carbohydr. Res.* **1994**, *264*, 1.
(25) Kirschner, K. N.; Woods, R. J. *J. Phys. Chem. A* **2001**, *105*, 4150.
(26) McCarren, P. R.; Gordon, M. T.; Lowary, T. L.; Hadad, C. M. *J. Phys. Chem. A* **2001**, *105*, 5911.
(27) Evdokimov, A. G.; Martin, J. L.; Kalb, J. *J. Phys. Chem. A* **2000**, *104*, 5291.
(28) Houseknecht, J. B.; McCarren, P. R.; Lowary, T. L.; Hadad, C. M. *J. Am. Chem. Soc.* **2001**, *123*, 8811.
(29) Cramer, C. J.; Truhlar, D. G. *J. Am. Chem. Soc.* **1993**, *115*, 5745.
(30) Ma, B.; III, H. F. S.; Allinger, N. L. *J. Am. Chem. Soc.* **1998**, *120*, 3411.
(31) Heidbrink, J. L.; Thoen, K. K.; Kenttämaa, H. I. *J. Org. Chem.* 2000, *63*, 645.
(32) Perez, J.; Petzold, C. J.; Watkins, M. A.; Vaughn, W. E.; Kenttämaa, H. I. *J. Am. Soc. Mass Spectrom.* **1999**, *10*, 1105.
(33) Perez, J.; Ramirez-Arizmendi, L. E.; Petzold, C. J.; Guler, L. P.; Nelson, E. D.; Kenttämaa, H. I. *Int. J. Mass Spectrom.* **2000**, *198*, 173.
(34) Marshall, A. G.; Wang, T. C. L.; Ricca, T. L. *J. Am. Chem. Soc.* **1985**, *107*, 7893.
(35) Frisch, M. J.; Trucks, G. W.; Schlegel, H. B.; Scuseria, G. E.; Robb, M. A.; Cheeseman, J. R.; Zakrzewski, V. G.; Montgomery, J. A., Jr.; Stratmann, R. E.; Burant, J. C.; Dapprich, S.; Millam, J. M.; Daniels, A. D.; Kudin, K. N.; Strain, M. C.; Farkas, O.; Tomasi, J.; Barone, V.; Cossi, M.; Cammi, R.; Mennucci, B.; Pomelli, C.; Adamo, C.; Clifford, S.; Ochterski, J.; Petersson, G. A.; Ayala, P. Y.; Cui, Q.; Morokuma, K.; Malick, D. K.; Rabuck, A. D.; Raghavachari, K.; Foresman, J. B.; Cioslowski, J.; Ortiz, J. V.; Baboul, A. G.; Stefanov, B. B.; Liu, G.; Liashenko, A.; Piskorz, P.; Komaromi, I.; Gomperts, R.; Martin, R. L.; Fox, D. J.; Keith, T.; Al-Laham, M. A.; Peng, C. Y.; Nanayakkara, A.; Challacombe, M.; Gill, P. M. W.; Johnson, B.; Chen, W.; Wong, M. W.; Andres, J. L.; Gonzalez, C.; Head-Gordon, M.; Replogle, E. S.; Pople, J. A.; *Gaussian 98, Revision A.7*; Gaussian, Inc.: Pittsburgh, 1998.
(36) Burkert, U.; Allinger, N. L.; Editors *ACS Monograph, No. 177: Molecular Mechanics*, 1982.
(37) Dewar, M. J. S.; Zoebisch, E. G.; Healy, E. F.; Stewart, J. J. P. *J. Am. Chem. Soc.* **1985**, *107*, 3902.
(38) James, K. L.; Angyal, S. J. *Austral. J. Chem.* **1972**, *25*, 1967.
(39) Finch, P. *Carbohydrates: Structures, Syntheses and Dynamics*; Kluwer Academic Publishers: Netherlands, 1999.
(40) Thoen, K. K.; Gao, L.; Ranatunga, T. D.; Vainiotalo, P.; Kenttämaa, H. I. *J. Org. Chem.* **1997**, *62*, 8702.
(41) Brown, W. H.; Foote, C. S. *Organic Chemistry*, 2nd ed.; Saunders College Publishing: Orlando, 1998.
(42) Eliel, E. L.; Allinger, N. L.; Angyal, S. J.; Morrison, F. A. *Conformational Analysis*; J. Wiley and Sons: New York, 1965.
(43) Juaristi, E.; Cuevas, G. *Tetrahedron* **1992**, *48*, 5019.
(44) Reeves, R. E. *J. Am. Chem. Soc.* **1950**, *72*, 1499.